Isotopomer-Selective Overtone Spectroscopy of Jet-Cooled Benzene by Ionization Detected IR + UV Double Resonance: The $N = 2$ CH Chromophore Absorption of $^{12}C_6H_6$ and $^{13}C^{12}C_5H_6$ near 6000 cm^{-1}

Michael Hippler,* Robert Pfab, and Martin Quack*

Physical Chemistry, ETH Zürich, CH-8093 Zürich, Switzerland

Received: April 30, 2003; In Final Form: October 1, 2003

Employing our recently introduced IR + UV double resonance scheme for obtaining mass-resolved infrared spectra, we have recorded the isotopomer selected $N = 2$ CH chromophore absorption of $^{12}C_6H_6$ and $^{13}C^{12}C_5H_6$ near 6000 cm^{-1} in a supersonic jet expansion of the benzene isotopomer mixture at natural abundance. The $^{13}C^{12}C_5H_6$ spectra are the first of this kind reported in the literature. For $^{13}C^{12}C_5H_6$, a preliminary analysis yields an approximate decay time of vibrational excitation $\tau \geq 130$ fs, which is presumably due to strong anharmonic Fermi resonances between CH-stretching and CH-bending modes. The $^{12}C_6H_6$ spectrum is compatible with a proposed model of intramolecular vibrational redistribution with a distinct hierarchy of time scales: the CH-stretching state is the IR chromophore state coupled to the IR field. With a decay time of $\tau \approx 100$ fs, vibrational excitation is redistributed to a first tier of vibrational states, probably CH-stretching/bending combination bands coupled by strong Fermi resonances. Vibrational excitation is then further redistributed with $\tau \approx 0.35$ ps to a second tier of states by weaker anharmonic resonances. The observed line widths give a lower bound for the decay time into the dense background manifold, $\tau > 1.3$ ps. Although the experimental jet spectra of $^{12}C_6H_6$ are in qualitative agreement with previously published calculated spectra, they disagree in finer details.

1. Introduction

Benzene has been a prototype molecule for many aspects of chemical structure and dynamics for much more than a century, including during the last five decades the dynamics of radiationless transitions from excited electronic states.[1−9] In particular, the use of the experimental technique of single vibronic level fluorescence developed by Parmenter and his school and then applied also by many others has led to much insight into processes of intramolecular vibrational redistribution (IVR) in electronically excited states.[10−15] There has also been substantial recent interest in the rovibrational dynamics of high Rydberg states of benzene.[16,17] Because of its high symmetry and special electronic structure, benzene is also prototypical for structural studies,[18−26] vibrational spectra and force fields,[18−20,28,29] and intramolecular vibrational redistribution in the electronic ground state.[30−50] Benzene has also been the prototype molecule for studies of local and normal mode behavior of its CH chromophore absorption (see also ref 32 for the historical development of these ideas).[37,41,51−54]

Benzene vibrational spectroscopy has thus a long tradition. Beginning with the vibrational assignment and calculation of normal modes by Wilson[18] and with the first comprehensive study on the vibrational spectroscopy of benzene and several deuterium labeled benzenes by Ingold and co-workers,[21] the fundamental vibrations of benzene $^{12}C_6H_6$ and several deuterium and ^{13}C-isotopomers are now fairly well characterized (see refs 20, 23−25, 29, 55−64 and references cited within). Employing these experimental data and additional ab initio corrections, Gauss and Stanton have recently obtained the equilibrium r_e structure of benzene with an approximate combined experimental-theoretical method,[26] somewhat similar to the more accurate approaches developed for $(HF)_2$ and CH_4.[27] The study of dynamic IVR processes in benzene has been greatly influenced by the pioneering work of Bray and Berry on the overtone spectroscopy of benzene, observed by grating and photoacoustic spectroscopy in a room-temperature cell.[40,41] After an approximate deconvolution to correct for the rotational band contour, the remaining broadening of overtone bands was attributed to ultrafast IVR decay processes. Sibert et al. explained this broadening by strong Fermi resonances between the CH-stretching oscillator and CH-bending modes as the main mechanism of IVR[42] (see also ref 43, ref 30 and the earlier proposal of this mechanism in the case of CX_3H molecules[65,66]). Although recent jet measurements have clearly shown that room-temperature spectra are heavily affected by inhomogeneous rotational and vibrational hot-band congestion,[36−39,57] classical and quantum calculations have established the dominant role of these Fermi resonances for IVR on very fast time scales.[42−50] The analysis of the IR active CH-stretching fundamental ν_{20} (Wilson notation[18,20]) in $^{12}C_6H_6$ has confirmed the presence of strong Fermi resonances by experiment.[37,57,59] The calculations predict even finer details of IVR in $^{12}C_6H_6$, and a whole sequence of time scales for redistribution of vibrational excitation among different modes has been suggested in recent publications.[42−50] A comparison of calculated spectra with the few available jet overtone spectra of $^{12}C_6H_6$, however, shows at most qualitative, but no quantitative, agreement. Compared to $^{12}C_6H_6$, only a few spectra of the isotopomer $^{13}C^{12}C_5H_6$ have been reported,[23,56,63,64] and no overtone spectra at all are published to our knowledge. Experimental data for $^{13}C^{12}C_5H_6$ would be relevant for structural studies, because isotopic substitution in

* Corresponding authors. E-mail addresses: hippler@ir.phys.chem.ethz.ch. martin@quack.ch.

10.1021/jp0305640 CCC: $25.00
Published on Web 11/15/2003

the carbon ring will provide structural information not available by deuterium labeling. Experimental ^{13}C-isotope shifts are also useful for force-field determinations. In a recent time-dependent quantum mechanical study of IVR from the second CH-stretching overtone in $^{12}C_6H_6$, nonstatistical energy redistribution has been attributed to the influence of the symmetry of the molecule.[48] It would thus be interesting to study the effect of the reduced symmetry in $^{13}C^{12}C_5H_6$ on IVR. The shift of vibrational states in $^{13}C^{12}C_5H_6$ compared to $^{12}C_6H_6$ will also affect Fermi and other anharmonic resonances and thus influence IVR processes. Such studies, however, are hindered by the lack of experimental spectra: in conventional spectroscopy on the natural benzene isotopomer mixture, $^{13}C^{12}C_5H_6$ absorption features are weak due to the low natural abundance (6.2%) and obscured by much stronger absorptions of the dominant $^{12}C_6H_6$. Isotopically enriched or pure $^{13}C^{12}C_5H_6$ is only available at great expense.

In even more general terms, our approach to the short-time (subfemtosecond to nanosecond) vibrational dynamics of polyatomic molecules[32,67] relies on the development of appropriate experimental tools, which allow us to unravel the often very complex spectra that arise from IVR in polyatomic molecules. For example, extensive hot-band transitions are to be expected for the overtone transitions of benzene, which will require jet-cooling to obtain vibrationally resolved spectra. The resulting low number densities in conjunction with low absorption cross-sections will therefore necessitate very sensitive detection of the IR excitation. To observe spectra of a selected species in an isotopomer mixture, the detection scheme must also be highly selective. The technique of isotopomer selective overtone spectroscopy (ISOS) recently introduced by us is ideally suited for this purpose.[68] In this scheme, vibrationally excited molecules are ionized by resonantly enhanced two-photon ionization via hot-bands of the stable intermediate S_1 electronic state. Compared to previous schemes, such a quasi-continuum of resonance enhancing intermediate states has the distinct advantage that the UV laser does not have to be scanned simultaneously with the IR laser during an infrared scan, because the resonance condition is always fulfilled. Ion detection in a mass spectrometer then allows one to obtain mass-selective spectra in a jet expansion; hot-band and isotopomer congestion are thus removed simultaneously. This scheme for mass-selective IR spectroscopy supplements another ISOS variant introduced by us, where the intermediate state is dissociative (overtone spectroscopy by vibrationally assisted dissociation and photofragment ionization, OSVADPI).[69−71] In the combination of both schemes, ISOS can be applied most generally to the IR spectroscopy of molecules with dissociative or bound intermediate electronic states.

In the past, IR + UV double resonance schemes have been reported, which show some similarities with the present scheme: ion-dip spectroscopy has been applied by Page, Shen, and Lee to the overtone spectroscopy of benzene.[37] A loss of ionization yield is accomplished by depletion of ground-state molecules due to IR excitation or by depletion of molecules from the intermediate state S_1 by stimulated emission pumping into vibrational levels of S_0. IR spectra are observed as small dips in an immense ionization background and they thus suffer from poor signal-to-noise ratios. Page, Shen, and Lee have also applied an ionization enhancement scheme, where IR excited benzene molecules are UV ionized via selected (1+1) REMPI transitions close to the electronic origin of the $S_1 \leftarrow S_0$ transition.[37] The additional selection rules of the UV transition increase the selectivity of the IR + UV double resonance scheme

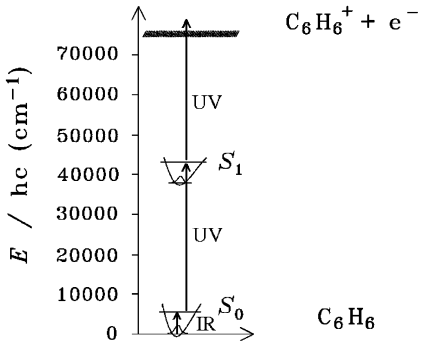

Figure 1. Scheme of excitation.

and thus aid the assignment of IR vibrational bands. As the UV ionization is via distinct, separated transitions, the UV laser has to be scanned simultaneously to keep the resonance during an IR scan. This is difficult to achieve, however, and no IR spectra obtained in this way have been reported. Recently, an IR + UV absorption scheme was presented, where vibrationally excited phenol was ionized by nonresonant two-photon ionization.[72] As discussed in our previous study,[68] however, ionization presumably also occurred in these cases by resonantly enhanced two-photon ionization, as in the present scheme, which is based on the original development of OSVADPI.[69−71]

Thus the aim of the present paper is to introduce the application of ISOS spectroscopy to benzene to unravel some aspects of IVR in this molecule and its isotopomer $^{13}C^{12}C_5H_6$ in the region of the $N = 2$ CH chromophore absorption around 6000 cm^{-1}. We refer here also to some of our studies of further isotopomers of benzene in relation to their vibrational dynamics.[73−75,96]

2. Experimental Section

Most aspects of the experimental setup employed to acquire IR + UV double resonance spectra have been described in our previous study of aniline.[68] In short, we excite benzene rovibrational levels with tunable IR laser radiation in a skimmed jet setup. The subsequent absorption of two UV quanta leads to the ionization of vibrationally excited molecules by resonantly enhanced two-photon ionization via the electronically excited state S_1. Figure 1 shows a survey of this scheme. IR idler radiation was generated in an optical parametrical amplifier (OPA) of a narrow-bandwidth dye laser operating at the signal wavelength. A frequency-tripled, injection-seeded Nd:YAG laser (Continuum, Powerlite 9010) pumped the OPA system (Lambda Physik, modified SCANMATE OPPO, 10 Hz repetition rate, 4 ns pulse length (full width at half-maximum, fwhm)). The spectra displayed here were recorded with an IR laser bandwidth of 0.15 cm^{-1}, because no additional structures were apparent with the improved bandwidth of 0.02 cm^{-1} achieved using an intracavity étalon in the dye laser in a series of control experiments at higher resolution. Employing a 25 cm focal length lens, the IR radiation with typically 1 mJ/pulse was focused into the core of a skimmed supersonic jet. Counter-propagating and with a delay of ca. 30 ns, the UV output of a frequency-doubled dye laser (Lumonics, HD-500) pumped by a frequency-doubled Nd:YAG laser (Continuum, NY82-10, with mode beating structure) with a typical pulse energy of 0.5 mJ/pulse was also focused to the same jet region by a 30 cm focal length lens. To avoid saturation of the transitions by IR excitation, the focus of the IR radiation was pulled slightly out of exact overlap with the jet region (by ca. 1−2 cm). Signals were then linearly dependent on the IR pulse energy, and the

ionization yield was IR power corrected assuming linear power dependence. IR frequency calibration was accomplished by simultaneously recording photoacoustic spectra of ca. 50 mbar methane in a reference cell. After a quadratic fit to methane reference lines with known positions,[76] an absolute wavenumber accuracy of 0.1 cm^{-1} is estimated for the data presented below.

Benzene (Fluka) was purified by distillation, and the purity was checked with gas chromatography. The natural isotopomer mixture contains about 6.4% of all ^{13}C isotopomers. Isotopically pure benzene $^{12}C_6H_6$ (depleted benzene, Cambridge Isotope Laboratories, CLM-867, ^{12}C 99.95%) was used without further purification for some FTIR measurements in comparison. For the jet experiments, 500 mbar of Ar as seed gas was flowing over frozen benzene at 0 °C, which has a vapor pressure of about 40 mbar.[77] The gas mixture then expanded into the probe vacuum chamber through the 1 mm circular orifice of a pulsed solenoid valve (General Valve) and a 0.5 mm skimmer at 3 cm distance. Ions resulting from IR and UV laser absorption were then mass analyzed in the time-of-flight mass spectrometer (custom-built Wiley/McLaren type reflectron, Kaesdorf, Munich).

Certain experimental conditions promoted the formation of clusters, for example, high partial benzene sample pressure, high Ar stagnation pressure, or probing molecules in the middle or at the end of the jet pulse train. Cluster formation became apparent by additional mass peaks in the TOF spectra and specific peaks in the UV spectrum of the $S_1 \leftarrow S_0$ transition in benzene. IR spectra of benzene clusters differ greatly from the monomer spectra.[37] Care was taken that the spectra displayed here were not affected by cluster formation. Reference spectra at room temperature were recorded with a high-resolution FTIR spectrometer (BOMEM DA002)[23,32,65] in a long path absorption cell (multipass White cell, Infrared Analysis). A resolution of 0.015 cm^{-1} was chosen (fwhm bandwidth, apodized), which is about twice the Doppler width at 300 K and 6000 cm^{-1} ($\sim$0.008 cm^{-1}). The spectrometer was equipped with a Globar light source, a CaF_2 beam splitter, and a liquid nitrogen-cooled InSb detector. Absolute wavenumber calibration of the FTIR spectra was accomplished by calibration against observed water lines of impurity water present in situ.[76] Sample pressures were measured with MKS Baratron capacitance gauges which had been calibrated, but no corrections were applied for loss due to adsorption at the cell walls during the measurement.

3. Results and Discussion

3.1. General Aspects. The absorption mechanism, which allows us to observe IR + UV double resonance signals in benzene (see Figure 1), is analogous to the scheme discussed in our previous work on aniline.[68] Without vibrational excitation, the UV radiation does not have sufficient energy to promote the transition to the electronically excited state S_1, which resonantly enhances ionization ((1+1) REMPI), and nonresonant two-photon ionization is also energetically not possible: Two-photon (1 + 1) REMPI ionization occurs via the $\tilde{A} \leftarrow \tilde{X}6_0^1$ transition and other vibronic levels of the S_1 $\tilde{A}$ state above 38 606 cm^{-1}.[2] One-photon 0_0^0 transitions to the *origin* of S_1 at 38 086 cm^{-1} are symmetry-forbidden in the electric-dipole approximation, but *vibronic* transitions of appropriate symmetry can be induced by vibrational excitation.[2] With an adiabatic ionization threshold at 9.2438 eV or 74 556 cm^{-1},[78] which is also close to the vertical ionization limit,[78] almost no benzene ions are observed under the present conditions applying UV radiation only below 37 280 cm^{-1} (about half the ionization threshold). Above that threshold, the ionization yield increases by nonresonant two-photon ionization. Below and slightly above that threshold, IR excitation of benzene enhances the ionization yield by several orders of magnitude, thus allowing very sensitive infrared excitation spectroscopy by IR + UV double resonance experiments. After IR excitation, Franck−Condon factors for hot-band transitions are much more favorable for the one-photon transitions to the S_1 state and the UV energy is sufficient to ionize vibrationally excited benzene molecules by resonantly enhanced two-photon ionization via vibrational hot-bands on the $S_1 \leftarrow S_0$ transition. For benzene with IR excitation at 6000 cm^{-1} and UV radiation at 37 600 cm^{-1}, the excess energy in S_1 is about 5500 cm^{-1}. At this energy, the vibrational density of states in the ground state S_0 is about 700 states per cm^{-1}, as calculated by the Beyer−Swinehart algorithm[79] using a set of observed fundamental frequencies compiled in refs 23 and 29. A similar density can be expected for the S_1 state. This corresponds to a dense set of states, which is accessible to one-photon excitation from the vibrationally excited electronic ground state. The ion yield in the IR + UV double resonance experiment is easily saturated by the UV pulse energies employed, and no variation in the ion yield is then apparent when the IR radiation is left resonant to a vibrational transition and the UV laser is scanned over an extensive range. The ionization yield therefore mirrors the IR excitation, and by scanning the IR laser, we obtain infrared spectra. Compared to results from ionization depletion detection schemes, the spectra are almost background free and have an excellent signal-to-noise ratio, even for the reduced number densities in a skimmed supersonic jet expansion. For the spectra shown below, an UV wavelength of 266 nm (37 594 cm^{-1}) was chosen for the IR + UV double resonance experiment. This particular UV wavelength would also be easily accessible and available by frequency quadrupling of a Nd:YAG laser, for example, by employing part of the output of the Nd:YAG laser, which is also used as a pump laser for the generation of IR radiation. Thus in this case the frequency-doubled dye laser would not be needed.

Although the ion yield in the present IR + UV experiment is sufficient to obtain ISOS spectra of benzene with good signal-to-noise ratio (see below), it is much lower than in our previous similar experiment with aniline.[68] Whereas the resonant $S_1 \leftarrow S_0$ absorption cross-section of benzene is comparatively large and easily saturated, the effective ionization cross-section of excited S_1 benzene is rather low.[80] This mismatch of cross-sections prevents efficient resonantly enhanced multiphoton ionization (compare also ref 81): De-excitation by stimulated emission and, in addition, intramolecular dynamic processes in excited S_1 benzene are expected to compete with UV photoionization and thus reduce the ionization yield in our scheme. The intramolecular dynamics of excited S_1 benzene has been studied extensively before: Above excess energies of 3000 cm^{-1}, Callomon et al. noticed the diffuseness of vibrational bands due to a sudden increase of intramolecular decay rates,[2] which has been attributed to some unknown nonradiative electronic relaxation mechanism ("channel three").[5] Since then, this unusual dynamic behavior has been studied in detail using experimental techniques such as "chemical timing" (O_2-pressure dependence of emission spectra),[15] rotationally resolved high-resolution spectroscopy,[7] or time-resolved photoionization experiments.[8,9] The high-resolution studies revealed a strong rotational dependence of the nonradiative decay rate.[7] These findings may be explained by a mechanism where very fast IVR occurs from bright rovibronic states to S_1 background states induced by rotationally dependent Coriolis and anharmonic couplings.[7,82] These S_1 background states may then undergo

rapid internal conversion to S_0, possibly aided by a conical intersection of the S_1 and S_0 potential energy surfaces.[7,9,82−84] After internal conversion, isoenergetic S_0 states are expected to have low ionization cross-sections due to small Franck−Condon factors to the ionization continuum.[8,9] It is not yet clear to which extent these dynamic processes reduce the ionization efficiency in the present scheme, because different S_1 states than previously studied are accessed by the IR + UV double resonance absorption. It is clear, however, that under the present experimental conditions ionization can compete successfully with the fast intramolecular relaxation, because photoionization is observed. It would be interesting to study in future experiments the intramolecular dynamics of highly excited states in S_1, which can be accessed by the IR + UV double resonance absorption with appropriate time resolution. However, the goal of the present study is obviously ground-state dynamics.

Benzene ionized by the IR + UV scheme used here has a characteristic mass spectrum, which is dominated by the parent ion and some weaker fragment ion peaks ranging from $C_{x=2-6}H_{y=0-5}$ to C. Obviously, some fragmentation occurs after ionization, because the UV wavelength and intensity chosen are not suitable for efficient resonantly enhanced or nonresonant multiphoton ionization of neutral C atoms or other fragments. By gating ionization detected IR excitation to the parent ion mass peak, mass-selective IR spectra are obtained. With a natural abundance of 1.1% ^{13}C, the benzene isotopomer $^{13}C^{12}C_5H_6$ with one ^{13}C atom has 6.2% abundance in the natural isotopomer mixture. A distinct shift of vibrational frequencies of the CH chromophore (and also in other modes[23,56,63,64]) is expected with this substitution. Mass gating the ionization detection in the IR + UV double resonance experiment at $m/z = 78$ and 79 u allows us to obtain the separate vibrational spectra of the two isotopomers $^{12}C_6H_6$ and $^{13}C^{12}C_5H_6$ in a single scan of the natural isotopomer mixture.

Benzene $^{12}C_6H_6$ (D_{6h} symmetry) has 20 normal vibrations, of which 10 are doubly degenerate.[18] For a summary of these fundamentals and the correlation of their numbering in Wilson's and Herzberg's notation we refer to ref 23. In D_{6h} symmetry, only perpendicular IR transitions from the ground state to E_{1u} vibrational states are allowed with an in-plane electric dipole transition moment, or parallel IR transitions to A_{2u} vibrational states with an out-of-plane transition moment.[20,23] Seven fundamental vibrations are Raman active and four are IR active.[18] Benzene has four fundamental normal modes between 3048 and 3074 cm^{-1}, which are essentially CH-stretching modes (in Wilson notation[18,20]): ν_2 (A_{1g} symmetry), ν_7 (E_{2g}), ν_{13} (B_{1u}), and the only IR active CH-stretching fundamental ν_{20} (E_{1u}). In the region of the first CH-stretching overtone near 6000 cm^{-1}, only the three combination bands of CH-stretching modes $\nu_{20} + \nu_7$, $\nu_7 + \nu_{13}$, and $\nu_2 + \nu_{20}$ have E_{1u} symmetry components and have thus allowed IR transitions from the ground state. All other combinations including the overtone $2\nu_{20}$ correspond to symmetry-forbidden transitions in the electric dipole approximation, excluding rovibrational coupling. As an alternative to the normal mode description of vibrational overtone bands, however, one may also use a local mode description[32,51−54] related to a set of normal mode combinations that are expected to be strongly coupled by Darling−Dennison and further anharmonic resonances. In the local mode picture, one would expect in each CH-stretching overtone region only one dominant absorption feature corresponding to one local CH oscillator with all vibrational excitation. For the first overtone region, a calculation of the CH-stretching absorption spectrum by Iachello and Oss based on the algebraic "vibron" model has given three IR absorptions, at 6004, 6113, and 6128 cm^{-1}, with relative intensity 1, 0.0017, and 0.006, respectively.[85] A pure local mode description of overtones, however, is also not satisfactory: theoretical studies[42−50] and the analysis of the spectrum of the CH-stretching fundamental[37,57,59] show that CH-stretching modes are in addition strongly coupled with CH-bending modes by Fermi resonances exchanging one quantum of CH-stretching excitation with two quanta of CH-bending excitation. All vibrational modes of a given symmetry with common polyad quantum number N are thus strongly coupled and mixed by Fermi, Darling−Dennison, and further anharmonic resonances, where $N = \upsilon_s + 0.5\upsilon_b$; υ_s represents all CH-stretching and υ_b all CH-bending quantum numbers.[32] We will therefore refer to the IR absorption near 6000 cm^{-1} as the $N = 2$ CH chromophore absorption, instead of the more common "first CH-stretching overtone", for example.

The isotopomer $^{13}C^{12}C_5H_6$ is an asymmetric top of the point group C_{2v}. We use the axis convention of refs 25 and 73 with the C_2 axis equal to the z-axis and the y-axis in the ring plane. The asymmetry parameter $\kappa = 0.9157$ is close to 1;[23] the replacement of one ^{12}C by the ^{13}C isotope introduces only a small perturbation. In C_{2v} symmetry, many more fundamentals lead to IR transitions: Among the 30 normal vibrations, 27 vibrations of A_1, B_1, and B_2 symmetry species are IR active, and all modes are Raman allowed. We have previously presented a high-resolution analysis of the ν_{11} (B_2) out-of-plane fundamental of this isotopomer situated at 673.6092(2) cm^{-1}.[23] Isotopic labeling will also cause in principle an alteration of normal mode characters (mode scrambling). The perturbation of the ^{13}C, however, is so small that intensities in $^{13}C^{12}C_5H_6$ cannot be expected to deviate much from the corresponding transitions in $^{12}C_6H_6$, despite the relaxed IR selection rules, and the character of corresponding vibrational modes will also be similar. The ^{13}C isotopic substitution will as a rule introduce a minor frequency shift to lower wavenumbers. The overtone vibrations of the CH chromophore will probably resemble local diatomic CH oscillators. The relative energy shift of ^{13}CH-harmonic oscillator vibrations compared to a ^{12}CH-harmonic oscillator is about −0.3%.

3.2. Room-Temperature Overtone Spectra and Isotopic Shifts. The $N = 2$ CH chromophore absorption spectrum of benzene obtained by FTIR spectroscopy at room temperature is shown in Figure 2. The spectrum of $^{12}C_6H_6$ was obtained in an isotopically pure sample. Depleted benzene $^{12}C_6H_6$ is readily available, because it is used as solvent in NMR spectroscopy. For $^{13}C^{12}C_5H_6$, no isotopically pure sample was available. To obtain its spectrum, the depleted spectrum has been subtracted from the normal benzene spectrum, using appropriate weights, and rescaled. The difference spectrum is essentially due to the $^{13}C^{12}C_5H_6$ isotopomer. This manipulation, however, is subject to extra noise and possibly also to systematic errors and distortions. The difference spectrum can therefore only be considered as an approximation to the proper $^{13}C^{12}C_5H_6$ spectrum; in particular, the absorption cross-sections indicated in Figure 2 are only approximate. The room-temperature spectra improve upon previously published spectra of the natural benzene isotopomer mixture, which had been obtained at much lower instrumental bandwidth (6−12 cm^{-1}).[41] The $^{13}C^{12}C_5H_6$ isotopomer spectrum is the first such published spectrum in the $N = 2$ CH chromophore absorption region.

The integrated absorption cross sections[32]

$$G = \int_{5500\ cm^{-1}}^{6200\ cm^{-1}} \sigma(\tilde{\nu})\tilde{\nu}^{-1}\, d\tilde{\nu} \qquad (1)$$

for the spectra shown in Figure 2 are $G(C_6H_6) = 0.0077\ pm^2$,

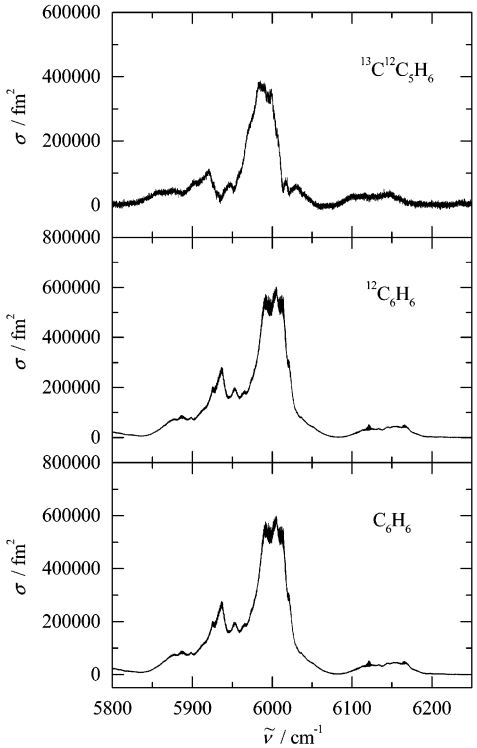

Figure 2. FTIR spectra of the $N = 2$ CH chromophore absorption of benzene at room temperature. The lower panel shows the spectrum of 2.20 mbar benzene (natural isotopomer mixture), the middle panel the corresponding spectrum of 2.14 mbar depleted benzene ($^{12}C_6H_6$, ^{12}C 99.95%) at room temperature ($l = 28$ m, resolution 0.015 cm^{-1}). In the upper panel, the depleted spectrum has been subtracted from the normal benzene spectrum using appropriate weights, and rescaled. This difference spectrum is essentially due to the $^{13}C^{12}C_5H_6$ isotopomer (note that absorption cross-sections for $^{13}C^{12}C_5H_6$ are only approximate).

$G(^{12}C_6H_6) = 0.0077$ pm^2, and $G(^{13}C^{12}C_5H_6) \approx 0.0050$ pm^2, where the last value is very approximate only. It should be stressed that no corrections were applied for loss of partial pressure due to adsorption of sample at the cell walls, etc. Thus we give these values only as rough indications of the absorption strengths and not as definitive values for the integrated band strengths, and we provide no uncertainty estimates for these values (the uncertainty is expected to be larger than 30%). The values quoted above can be translated into an electric dipole transition moment by[32]

$$(G/\mathrm{pm}^2) = 41.624|M_{\mathrm{fi}}/\mathrm{D}|^2 \qquad (2)$$

resulting in $|M_{\mathrm{fi}}| = 0.014$ D for C_6H_6 and $^{12}C_6H_6$, which is of the order of magnitude expected for the local CH Morse oscillator with a Mecke-dipole model function.[32,86−89] Earlier measurements of $N = 2$ polyad band strengths in C_6H_6 resulted in $G = 0.0077$ pm^2 (ref 90) and $G = 0.0098$ pm^2 (ref 41), in good agreement with the present value considering the usual uncertainties. More accurate results could be obtained by measuring the band strengths at a well-defined constant vapor pressure over a thermostated reservoir.[91] The approximation of a conservation of the chromophore electric dipole transition moment under a change of internal energy by jet cooling can in principle be used to translate the relative signal strengths reported below for the jet ISOS spectra into absolute absorption cross sections.

The general appearance of both isotopomer spectra at room temperature is similar. A main broad feature with a width of

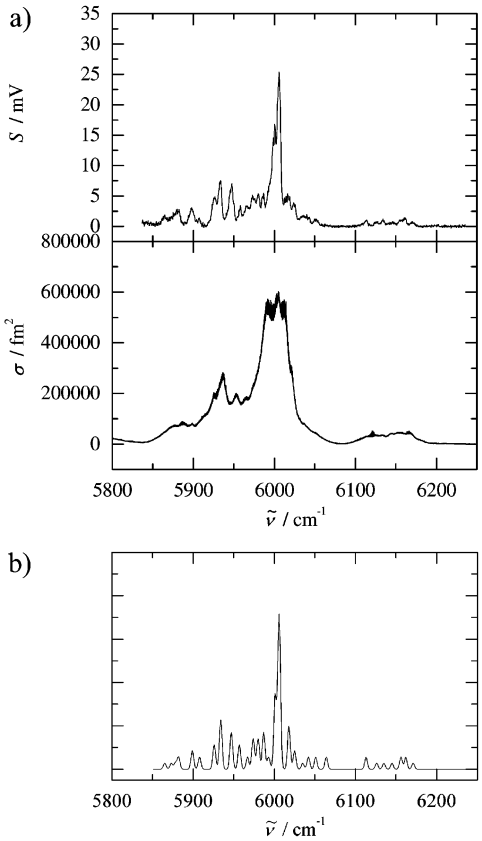

Figure 3. $N = 2$ CH chromophore absorption of $^{12}C_6H_6$ near 6000 cm^{-1}. (a) The lower panel shows an FTIR reference spectrum of 2.14 mbar depleted benzene ($^{12}C_6H_6$, ^{12}C 99.95%) at room temperature ($l = 28$ m, resolution 0.015 cm^{-1}). The upper panel shows the ionization detected ISOS spectrum of jet-cooled benzene, mass gated at $m/z = 78$ u ($^{12}C_6H_6$), in a jet-expansion with 500 mbar of Ar. (b) Synthetic jet spectrum reconstructed from the data of Page, Shen, and Lee,[37] with intensities corrected for saturation. Note that the corresponding experimental spectrum has in addition significant noise.[37]

ca. 40 cm^{-1} (fwhm) with a distinct central peak and some diffuse irregular structure dominates the spectrum. The central peak is at 6005.3 ± 0.4 cm^{-1} for $^{12}C_6H_6$ and at 5991 ± 1 cm^{-1} for $^{13}C^{12}C_5H_6$. Higher CH-stretching overtones of $^{12}C_6H_6$ are well described by a Morse oscillator with $\omega_m = 3163$ cm^{-1} and $x_m = 57.7$ cm^{-1}, which has been interpreted as the local mode ^{12}-CH oscillator absorption.[36,41] The ^{12}CH Morse oscillator vibration for $v = 2$ is then calculated at 5980 cm^{-1}, and at 5963 cm^{-1} for the ^{13}CH Morse oscillator taking into account the change of reduced masses.[41] The calculated estimated ^{13}C-isotopomer shift is −17 cm^{-1} or −0.29%. A closer examination of the experimental spectra reveals some differences in relative intensities and rotational band contours of corresponding transitions, for example, in the wing at higher wavenumbers of the main feature, where two additional features are apparent for $^{13}C^{12}C_5H_6$. A further assignment or interpretation of the room-temperature spectra is not possible because of inhomogeneous structure and congestion. In addition to broad rotational contours, room-temperature spectra are heavily affected by vibrational hot-band transitions, because about 40% of benzene molecules are in vibrationally excited states.

3.3. ISOS Jet-Cooled Overtone Spectra and Isotopic Shifts. In Figures 3a and 4, the ionization detected ISOS spectra of benzene in a jet-expansion with 500 mbar of Ar are displayed and compared with the corresponding FTIR room-temperature spectra. An UV wavelength of 266 nm (37 594 cm^{-1}) was chosen for the IR + UV ionization. In the natural benzene

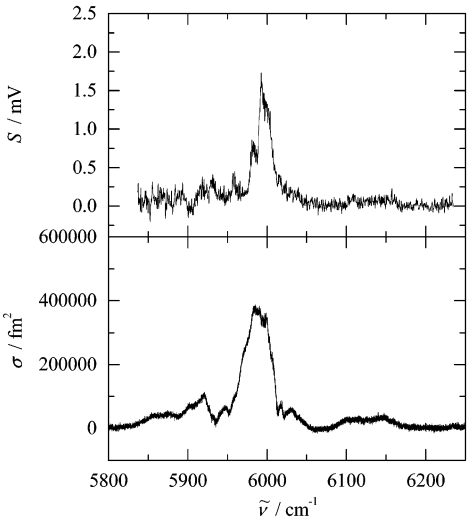

Figure 4. $N = 2$ CH chromophore absorption of $^{13}C^{12}C_5H_6$ near 6000 cm^{-1}. The lower panel shows a manipulated spectrum, where the FTIR spectrum of 2.14 mbar depleted benzene ($^{12}C_6H_6$, $^{12}C_6$ 99.95%) at room temperature has been subtracted from the FTIR spectrum of 2.20 mbar benzene (natural isotopomer mixture) and rescaled ($l = 28$ m, resolution 0.015 cm^{-1}). The difference spectrum is essentially due to the $^{13}C^{12}C_5H_6$ isotopomer (as in Figure 2). The upper panel shows the ionization detected ISOS spectrum of jet-cooled benzene, mass gated at $m/z =$ 79 u ($^{13}C^{12}C_5H_6$), in a jet-expansion with 500 mbar of Ar.

isotopomer mixture, mass gating the ionization detection at $m/z = 78$ u and 79 u yielded simultaneously the separate jet-cooled IR spectra of $^{12}C_6H_6$ and $^{13}C^{12}C_5H_6$ isotopomers, respectively. In comparable jet experiments on aniline,[68] rotational temperatures of about 5 K have been obtained, and vibrational hot-band transitions have been almost completely suppressed; similar conditions are expected to apply here. The spectral simplification obtained by jet-cooling is striking. The width (fwhm) of vibrational band contours decreases from about 40 cm^{-1} at room temperature to about 4 to 5 cm^{-1} for $^{12}C_6H_6$, and distinct resolved or partly resolved vibrational transitions become apparent. Tables 1 and 2 provide a listing of the positions and intensities of observed transitions in the jet-cooled $N = 2$ CH chromophore absorption spectra of the $^{12}C_6H_6$ and $^{13}C^{12}C_5H_6$ isotopomers. The $^{12}C_6H_6$ spectrum (Figure 3a) is essentially in good agreement with the previously published jet spectrum of Page, Shen, and Lee,[37] but it is not affected by saturation and has a better signal-to-noise ratio. In the detailed comparison, some differences in band contours and intensities are noticed, however, which are presumably due to different rotational temperatures, the improved laser bandwidth in the present study (0.15 cm^{-1} compared to 1 cm^{-1}), and the effects of saturation in the previous investigation (see Figure 3b for a comparison of line positions and corrected relative intensities). The jet-cooled spectrum of the $^{13}C^{12}C_5H_6$ isotopomer in Figure 4 is reported here for the first time. It demonstrates that the 6.2% abundance in the natural isotopomer mixture of benzene is sufficient to obtain jet spectra with the new ISOS technique. The strongest peak in the $^{12}C_6H_6$ jet spectrum is located at 6006.0 $\pm$ 0.5 cm^{-1}, and the corresponding strongest peak in the $^{13}C^{12}C_5H_6$ jet spectrum at 5993 $\pm$ 1 cm^{-1}. These peak positions provide good estimates for the band origins. A ^{13}C-isotopomer shift of -13 cm^{-1} or a relative shift of -0.22% is thus deduced, which is close to the estimate from the room-temperature spectrum, but much more reliable, because the value has been obtained from vibrational bands with much reduced inhomogeneous congestion. In $^{12}C_6H_6$, the main absorption feature and other features have a width (fwhm) of about 4$-$5 cm^{-1}, whereas spectral contours in $^{13}C^{12}C_5H_6$ are much broader: from lower to higher wavenumbers, the main absorption feature and the peak before that feature have a contour with a sharp rise in intensity, then a slowly decreasing intensity followed by a sharp decline. The entire bandwidth (fwhm) is about 15 cm^{-1}, but the sharp edges have a half-width of about 4 cm^{-1} only. It is thus likely that part of the broadening is due to spectral congestion, for example, by the different rotational contour of the asymmetric rotor or by the presence of additional vibrational bands that are IR active in the C_{2v} symmetry or arise through further allowed anharmonic and rovibrational couplings.

TABLE 1: Peak Positions in the Jet-Cooled $N = 2$ CH-Stretch Overtone Spectra of the $^{12}C_6H_6$ Benzene Isotopomer (Compare Figure 3a)

peak no.	position/cm^{-1} [a]	intensity/mV[b]	remarks[c]
(a) Weak and Medium Strong Features at Lower Wavenumbers			
1	5864.8	1.9	broad
2	5880.1	2.8	broad
3	5897.7	3.1	
4	5907.5	1.4	
5	5924.5	4.8	overlapped with no. 6
6	5933.6	7.5	overlapped with no. 5
7	5947.8	7.0	
(b) Overlapped Features in the Envelope of the Main Absorption near 6006 cm^{-1}			
8	5956.4	2.7	
9	5958.5	3.4	
10	5966.6	3.3	broad
11	5973.8	4.9	broad
12	5979.7	5.4	
13	5985.4	4.9	
14	5986.8	5.5	
15	5998.9	14.5	
16	6000.4	16.8	
17	6005.1	23.6	
18	6006.0	25.4	maximum
19	6012.6	4.7	
20	6014.6	4.9	
21	6016.4	5.3	
22	6018.9	4.9	
23	6023.7	3.8	broad
24	6038	1.5	very broad
25	6052	1.2	very broad
(c) Weak Features at Higher Wavenumbers			
26	6113.6	1.1	
27	6126.0	0.6	
28	6134.2	1.1	
29	6146	0.7	very broad
30	6156.2	1.0	overlapped with no. 31
31	6161.6	1.4	overlapped with no. 30
32	6170.1	0.8	

[a] Peak position, estimated accuracy ± 0.5 cm^{-1}. [b] Peak intensity in the ISOS spectrum (compare Figure 3a). [c] Normal features have a fwhm of about 4$-$5 cm^{-1}, broad features ca. 10 cm^{-1}, and very broad features 15$-$20 cm^{-1}.

TABLE 2: Peak Positions in the Jet-Cooled $N = 2$ CH-Stretch Overtone Spectra of the $^{13}C^{12}C_5H_6$ Benzene Isotopomer (Compare Figure 4)

peak no.	position/cm^{-1} [a]	intensity/mV[b]
1	5918	0.3
2	5931	0.4
3	5958	0.45
4	5981	0.9
5	5993	1.7
6	6108	0.17
7	6102	0.14

[a] Peak position, estimated accuracy ± 1 cm^{-1}. [b] Peak intensity in the ISOS spectrum (compare Figure 4).

A degenerate E_{1u} IR active vibrational band in D_{6h} symmetry correlates to two IR active bands of A_1 and B_1 species in C_{2v} symmetry,[20] which may be coupled by a strong Coriolis interaction.[56] This effect may also give rise to an anomalous intensity distribution.

3.4. Intramolecular Vibrational Redistribution. A detailed description of IVR processes in the $N = 2$ CH chromophore absorption could be obtained, if the character of all absorption features could be assigned in terms of both effective and full molecular Hamiltonians.[67] This is not feasible at present. Previous theoretical studies, however, provide some guidelines for a tentative statistical interpretation of the $^{12}C_6H_6$ jet spectrum: The calculations of Iachello and Oss have shown that one strong pure CH-stretching transition prevails in the IR spectrum of this region, which is calculated to occur at 6004 cm^{-1}.[85] This CH-stretching mode is coupled to the IR field as a chromophore state. By anharmonic coupling, its vibrational excitation will be redistributed among many vibrational modes, giving rise to the observed vibrational bands in the IR jet spectrum. At 6000 cm^{-1}, the vibrational density of states is about 1560 states per cm^{-1}, as counted in the harmonic approximation by the Beyer−Swinehart algorithm[79] using an experimental set of fundamental vibrations (compiled in refs 23 and 29). E_{1u} symmetry is required for an allowed anharmonic coupling with the E_{1u} CH-stretching overtone level. In the regular limit,[92] the density of E_{1u} states is $2/24 = 1/12$ of the total density, about 130 states per cm^{-1} (note that in the total density of states, vibrations are multiplied according to their degeneracy, whereas in the density of vibrational states of a given symmetry species, degenerate vibrational levels are counted as single levels). If the off-diagonal coupling matrix elements are uncorrelated and of the order of or larger than the mean energy between consecutive coupled states, a Lorentzian with fwhm $\tilde{\Gamma}$ centered around the chromophore state envelops a series of absorption lines, indicating exponential decay of vibrational excitation from the chromophore state to the background states with decay time $\tau = h/2\pi\Gamma = 1/2\pi c\tilde{\Gamma}$ (Lorentzian width Γ in energy units, $\tilde{\Gamma}$ in wavenumber units).[30,93] Instead of the one-step coupling of the bright state to the bath, a sequential "tier" picture[30,31,34,35,41] appears to provide a better description of IVR in benzene: In a first tier, the bright CH-stretching state is strongly coupled to a subset of vibrational states. A broad Lorentzian curve obtained by a visual fit envelops all absorption features observed in the experimental jet spectrum (Figure 5a, dotted curve) with fwhm $\tilde{\Gamma} = 45$ cm^{-1}, corresponding to a decay time of vibrational excitation into a first tier of vibrational states of $\tau \approx 120$ fs. Because CH-stretching and -bending modes are known to be coupled by strong Fermi resonances,[32,37,42−50,57,60] the first tier presumably involves the CH-stretching/bending combination bands of E_{1u} symmetry species in the absorption region. The inferred decay time is compatible with theoretical calculations[42−50] and with typical redistribution times found, e.g., for CH-stretching/bending Fermi resonances in CHX_3 or $CHXY_2$ compounds.[32,33,65,66] The Lorentzian is centered at 5988 cm^{-1}, which corresponds to the position of the chromophore state. Higher CH-stretching overtones are well described by a Morse oscillator, which has been interpreted as the local mode CH oscillator absorption.[36,41] It is interesting to note that the Morse oscillator level $v = 2$ is calculated at 5980 cm^{-1}, close to the position found here for the chromophore state in the $N = 2$ polyad absorption. The main absorption feature at 6006 cm^{-1} has accompanying weaker satellite lines. A second Lorentzian obtained by a visual fit envelops these absorption features (Figure 5a), dashed curve) with $\tilde{\Gamma} = 15$ cm^{-1} corresponding to a decay time $\tau \approx 0.35$ ps of vibrational excitation into a second tier of vibrational states. This tier could be composed of vibrational states coupled by weaker anharmonic resonances to the CH-stretching/bending manifold. The two-tier statistical model proposed here for IVR in the $N = 2$ CH chromophore absorption is compatible with the experiment and with expectation. The analysis of the CH-stretching fundamental has provided a similar coupling scheme:[37,57,60] the IR-active CH-stretching fundamental ν_{20} is coupled to the IR field. By strong Fermi resonances with CH-stretching/bending combination bands, vibrational excitation is redistributed to an absorption triad, ν_{20}, $\nu_{18} + \nu_{19}$, and $\nu_1 + \nu_6 + \nu_{19}$. The latter band is in addition coupled by weaker anharmonic resonances with $\nu_3 + \nu_6 + \nu_{15}$. The 4 cm^{-1} width (fwhm) of features in the jet spectrum of the $N = 2$ absorption is an upper bound for the homogeneous bandwidth $\tilde{\Gamma}$ giving a lower bound $\tau > 1.3$ ps for the decay time of further redistribution of vibrational excitation. Callegari et al. have obtained the "eigenstate resolved" benzene spectrum between 6004 and 6008 cm^{-1} by IR−IR double resonance with continuous wave laser systems and bolometric detection.[38,39] From the observed clustering of eigenstates, the authors deduced further time scales for IVR ranging from 100 ps to 2 ns.

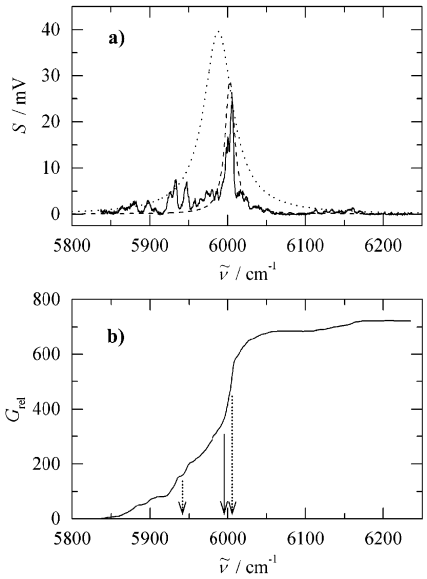

Figure 5. (a) Jet-cooled, isotopomer-selective overtone spectrum of the $N = 2$ CH chromophore absorption of $^{12}C_6H_6$ (as in Figure 3a). The dotted curve is a Lorentzian function with 45 cm^{-1} fwhm centered at 5988 cm^{-1}, and the dashed curve a Lorentzian function with 15 cm^{-1} fwhm centered at 6003 cm^{-1}. (b) Relative $G_{rel}(\tilde{\nu})$ (integral of the absorption cross section) corresponding to the jet-cooled $N = 2$ CH chromophore absorption of $^{12}C_6H_6$ (as in Figure 3a or Figure 5a), in arbitrary units. The position of the half-height (solid arrow) and of the quarter- and three-quarter-heights (dotted arrows) are indicated (see text for a discussion).

Another useful and more quantitative analysis[30] is possible by considering the quantity $S(\tilde{\nu})$,

$$S(\tilde{\nu}) = \int_{\tilde{\nu}_0}^{\tilde{\nu}} \sigma(\tilde{\nu}')\, d\tilde{\nu}' \tag{3}$$

or more appropriately, but almost equivalently,

$$G(\tilde{\nu}) = \int_{\tilde{\nu}_0}^{\tilde{\nu}} \sigma(\tilde{\nu}')\tilde{\nu}'^{-1}\, d\tilde{\nu}' \approx \frac{1}{\tilde{\nu}_G} S(\tilde{\nu}) \tag{4}$$

where the lower integration limit $\tilde{\nu}_0$ is near 5850 cm^{-1}, outside the absorption range, and $\tilde{\nu}_G$ is the center of gravity or effective

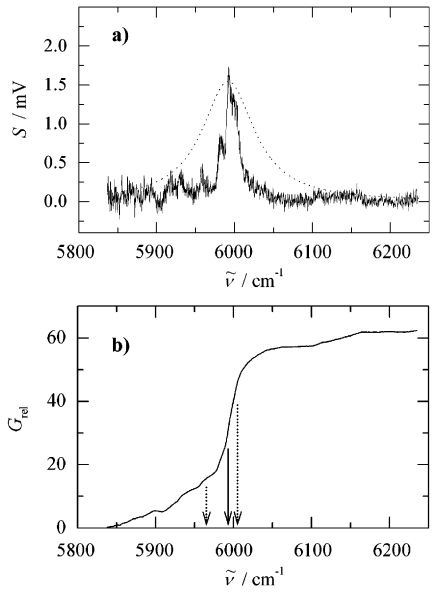

Figure 6. (a) Jet-cooled, isotopomer-selective overtone spectrum of the $N = 2$ CH chromophore absorption of $^{13}C^{12}C_5H_6$ (as in Figure 4). The dotted curve is a Lorentzian function with 40 cm^{-1} fwhm centered at 5993 cm^{-1}. (b) Relative $G_{rel}(\tilde{\nu})$ (integral of the absorption cross section) corresponding to the jet-cooled $N = 2$ CH chromophore absorption of $^{13}C^{12}C_5H_6$ (as in Figure 4 or Figure 6a), in arbitrary units. The position of the half-height (solid arrow) and of the quarter- and three-quarter-heights (dotted arrows) are indicated (see text for a discussion).

band center. $G(\tilde{\nu})$, corresponding to the jet-cooled $N = 2$ CH chromophore absorption of $^{12}C_6H_6$ (as in Figure 3a or Figure 5a), is shown in Figure 5b. The effective band center is obtained from the position of half-height of this function, whereas the effective widths are obtained from the quarter- and three-quarter-heights centered around this position. One obtains $\tilde{\nu}_G = 5995$ cm^{-1} for this chromophore absorption with width $\tilde{\Gamma} = 60$ cm^{-1}, in reasonable agreement with the visual fit shown in Figure 5a. We thus finally quote $\tilde{\Gamma} = 50 \pm 10$ cm^{-1} and a resulting approximate decay time of vibrational excitation $\tau \approx 100$ fs combining both approaches. The basis of this dynamic analysis is the assumption of one single chromophore absorption carrying all the oscillator strength in the integration range, an assumption that has had some theoretical basis for a long time[86,30−32] (see, in particular, the historical review in ref 32) and that has been justified again more recently, e.g., by the "vibron" model calculations of Iachello and Oss (ref 85, see also above). For $^{12}C_6H_6$, this chromophore absorption probably resembles the excitation of local ^{12}CH Morse oscillators.

Due to the similarities in the general appearance of the jet spectra, the $N = 2$ CH chromophore absorption of $^{13}C^{12}C_5H_6$ can probably be interpreted on similar general lines as outlined here for $^{12}C_6H_6$. Because no theoretical calculations exist to our knowledge to guide the assignment, only a preliminary analysis of the IVR dynamics can be made at this stage using some simple models: On the basis of a local mode picture, one could expect two chromophore absorptions for $^{13}C^{12}C_5H_6$ in this overtone region, a strong absorption due to local ^{12}CH Morse oscillators, and a weaker absorption due to the local ^{13}CH Morse oscillator. Assuming now that the absorption of the local ^{12}CH Morse oscillators is dominating, one can attempt a similar quantitative analysis as before for the $^{12}C_6H_6$ isotopomer: In Figure 6b, $G(\tilde{\nu})$ is shown for the jet-cooled $N = 2$ CH chromophore absorption of $^{13}C^{12}C_5H_6$. The effective band center is obtained at $\tilde{\nu}_G = 5993$ cm^{-1} with width $\tilde{\Gamma} = 40$ cm^{-1}, and

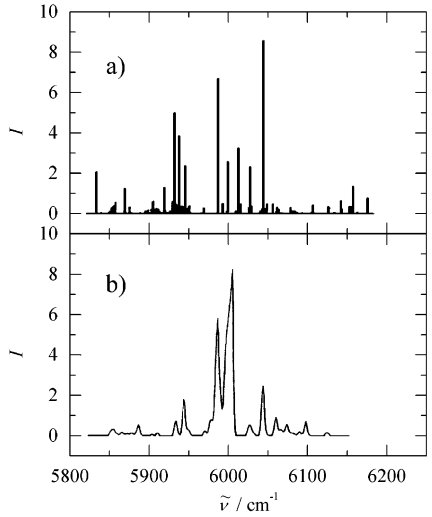

Figure 7. Previously published calculated spectra of benzene $^{12}C_6H_6$. (a) Stick spectrum, redrawn from Rashev, Stamova, and Djambova.[49] (b) Stick spectrum convoluted with rotational contours of 5 cm^{-1} fwhm, redrawn from Zhang and Marcus.[45]

a corresponding Lorentzian curve indeed envelops all absorption features of the $^{13}C^{12}C_5H_6$ jet spectrum (Figure 6a). The effective band center is very close to the value for $^{12}C_6H_6$, presumably because the dominating chromophore absorption is in both cases due to ^{12}CH Morse oscillators (strictly speaking, 3 types, the ^{13}CH Morse oscillator has an expected shift of -17 cm^{-1}). Because the inherent assumption of one single chromophore absorption in this analysis is presumably not strictly valid for $^{13}C^{12}C_5H_6$, the actual $\tilde{\Gamma}$ due to IVR will be somewhat smaller than the 40 cm^{-1} obtained by the integration method. We thus estimate $\tilde{\Gamma} \leq 40$ cm^{-1} and a resulting approximate decay time of vibrational excitation $\tau \geq 130$ fs. This very fast decay of initial vibrational excitation is most likely due to strong anharmonic Fermi resonances between CH-stretching and CH-bending modes, because similar resonances and redistribution times have been found for $^{12}C_6H_6$ (see above) and CHX_3 or $CHXY_2$ compounds.[32,33,65,66] A further and more detailed analysis of the $^{13}C^{12}C_5H_6$ jet spectrum has to await additional experimental and theoretical results to guide the assignment. In particular, a detailed analysis of the $N = 1$ CH chromophore absorption around 3050−3100 cm^{-1} should be feasible; it is anticipated to provide results that could help to unravel the analysis of the $N = 2$ absorption. Such studies are in progress, applying the new ISOS scheme to the spectroscopy of benzene isotopomers.

Zhang and Marcus[45] have calculated the absorption spectrum of $^{12}C_6H_6$ in the 6000 cm^{-1} region using an anharmonic force field together with dipole moment derivatives.[28] More recently, Rashev et al. have also published a calculated spectrum based on anharmonic force fields[28,29] and symmetrized complex coordinates.[49] Relative intensities in the stick spectrum were calculated by assuming local CH oscillators as zeroth-order "bright" states. Both calculated spectra are shown in Figure 7. A comparison with our experimental jet spectrum shows perhaps qualitative, but certainly not quantitative, agreement; also both calculations differ markedly. Because they are based on force fields, which were also used in theoretical IVR studies, this disagreement between theory and experiment casts also some doubt on the reliability of the corresponding theoretical calculations of IVR, in particular concerning details on longer time scales. Further progress in the understanding of IVR in the important model molecule benzene could be achieved by

alternative theoretical models to be developed in close comparison with experimental jet spectra. It would also be interesting to perform calculations based on the most recent anharmonic force field by Miani et al. [29]

4. Conclusions

The IR + UV double resonance scheme for obtaining mass-selective, jet-cooled infrared spectra has been introduced, where vibrationally excited benzene is ionized by resonantly enhanced two-photon ionization via hot-bands of the $S_1 \leftarrow S_0$ transition. Ionization detection in a time-of-flight mass spectrometer allows isotopomer-selective overtone spectroscopy (ISOS), thus combining high-resolution IR spectroscopy with mass resolution. Compared to ionization depletion schemes, the technique is virtually background free. It is highly selective and sensitive and thus has great potential for analytical applications. The technique was demonstrated on jet-cooled overtone spectra of benzene isotopomers, where it was possible to observe separate spectra of the $N = 2$ CH chromophore absorption near 6000 cm^{-1} for $^{12}C_6H_6$ and $^{13}C^{12}C_5H_6$ at natural abundance in the benzene isotopomer mixture. The $^{13}C^{12}C_5H_6$ jet spectra are the first of this kind reported in the literature. The main (peak) absorption shows an isotope shift of about -13 cm^{-1} whereas the center of gravity of the band is shifted by -2 cm^{-1}. Jet cooling is essential to remove much of the inhomogeneous hot-band congestion, which heavily affects room-temperature spectra. The absorption spectra show many vibrational bands that are to be interpreted as a signature of IVR due to anharmonic coupling of numerous vibrational states to one chromophore state. For $^{13}C^{12}C_5H_6$, a preliminary analysis yields an approximate decay time of vibrational excitation $\tau \geq 130$ fs, which is presumably due to strong anharmonic Fermi resonances between CH-stretching and CH-bending modes. The observed spectrum of $^{12}C_6H_6$ is compatible with a proposed model of IVR with a distinct hierarchy of time scales: the CH-stretching state is the IR chromophore state coupled to the IR field. With decay time $\tau \approx 100$ fs, vibrational excitation is redistributed to a first group of vibrational states, probably CH-stretching/bending combination levels coupled by strong Fermi resonances to the pure stretching chromophore. This gives rise to a broad absorption modulated by a Lorentzian with a width of 50 ± 10 cm^{-1} (fwhm) enveloping all absorption features. Vibrational excitation is then further redistributed with $\tau \approx 0.35$ ps to a second group of states, possibly coupled by weaker higher order anharmonic resonances of further levels coupled to the CH-stretching/bending manifold. A bound on homogeneous line widths of <4 cm^{-1} provides a bound for the decay time into the dense background manifold of $\tau > 1.3$ ps. This picture of sequential coupling is in agreement with the original general proposal in refs 30 and 31 and can be related to earlier findings on another prototype molecule for IVR, CF_3H, where such a sequential coupling with separate time scales is clearly visible in the analysis of the overtone spectra.[65,94,95] The experimental jet-cooled spectra of benzene $^{12}C_6H_6$ are in their general appearance somewhat similar to previously calculated spectra,[45,49] but they clearly disagree in many details. Thus a more complete understanding of IVR processes in the important prototype molecule benzene requires further theoretical and experimental work. A considerable simplification might be possible in a study of C_6D_5H by a similar approach.

Acknowledgment. We are grateful to Hans Hollenstein for substantial help and discussions. We enjoyed scientific exchange with Charlie Parmenter and stimulus in our work by him over more than three decades. Our work is supported financially by the ETH Zürich (including C4, CSCS and AGS) and the Schweizerischer Nationalfonds.

References and Notes

(1) Kistiakowsky, G. B.; Parmenter, C. S. *J. Chem. Phys.* **1965**, *42*, 2942.
(2) Callomon, J. H.; Dunn, T. M.; Mills, J. M. *Philos. Trans R. Soc. London A* **1966**, *259*, 499 and references therein.
(3) Stockburger, M. *Ber. Bunsen-Ges. Phys. Chem.* **1968**, *72*, 151.
(4) Jortner, J.; Rice, S. A.; Hochstrasser, R. M. *Adv. Photochem.* **1969**, *7*, 149.
(5) Callomon, J. H.; Parkin, J. E.; Lopez-Delgado, R. *Chem. Phys. Lett.* **1972**, *13*, 125. Parmenter, C. S. *Adv. Chem. Phys.* **1972**, *22*, 365. Riedle, E.; Neusser, H. J.; Schlag, E. W. *Faraday Discuss. Chem. Soc.* **1983**, *75*, 387. Callomon, J. H. *Faraday Discuss. Chem. Soc.* **1983**, *75*, 417.
(6) Avouris, P.; Gelbart, W. M.; El-Sayed, M. A. *Chem. Rev.* **1977**, *77*, 793.
(7) Riedle, E.; Neusser, H. J.; Schlag, E. W. *J. Phys. Chem.* **1982**, *86*, 4847. Riedle, E.; Weber, Th.; Schubert, U.; Neusser, H. J.; Schlag, E. W. *J. Chem. Phys.* **1990**, *93*, 967.
(8) Smith, J. M.; Zhang, X.; Knee, J. L. *J. Phys. Chem.* **1995**, *99*, 1768.
(9) Clara, M.; Hellerer, Th.; Neusser, H. J. *Appl. Phys. B* **2000**, *71*, 431.
(10) Parmenter, C. S.; Schuyler, M. W. *J. Chem. Phys.* **1970**, *52*, 5366.
(11) Knight, A. E. W.; Parmenter, C. S.; Schuyler, M. W. *J. Am. Chem. Soc.* **1975**, *97*, 1993, 2005.
(12) Atkinson, G. H.; Parmenter, C. S. *J. Mol. Spectrosc.* **1978**, *73*, 52.
(13) Quack, M.; Stockburger, M. *J. Mol. Spectrosc.* **1972**, *43*, 87.
(14) Parmenter, C. S. *Faraday Discuss.* **1983**, *75*, 7.
(15) Moss, D. B.; Parmenter, C. S. *J. Phys. Chem.* **1986**, *90*, 1011. Longfellow, R. J.; Moss, D. B.; Parmenter, C. S. *J. Chem. Phys.* **1988**, *92*, 5438.
(16) Neuhauser, R. G.; Siglow, K.; Neusser, H. J. *J. Chem. Phys.* **1997**, *106*, 896.
(17) Osterwalder, A.; Willitsch, S.; Merkt, F. *J. Mol. Struct.* **2001**, *599*, 163.
(18) Wilson, E. B. *Phys. Rev.* **1934**, *45*, 706; **1934**, *46*, 146.
(19) Herzberg, G. *Molecular spectra and Molecular Structure*; Van Nostrand: Toronto, 1945; Vol. II.
(20) Wilson, E. B.; Decius, J. C.; Cross, P. C. *Molecular Vibrations*; Dover Publications: New York, 1980.
(21) Angus, W. R.; Bailey, C. R.; Hale, J. B.; Ingold, C. K.; Leckie, A. H.; Raisin, C. G.; Thompson, J. W.; Wilson, C. L. *J. Chem. Soc. London* **1936**, 912.
(22) Tamagawa, K.; Iijima, T.; Kimura, M. *J. Mol. Struct.* **1976**, *30*, 243.
(23) Hollenstein, H.; Piccirillo, S.; Quack, M.; Snels, M. *Mol. Phys.* **1990**, *71*, 759.
(24) Plíva, J.; Johns, J. W. C.; Goodman, L. *J. Mol. Spectrosc.* **1991**, *148*, 427.
(25) Snels, M.; Beil, A.; Hollenstein, H.; Quack, M. *Chem. Phys.* **1997**, *225*, 107.
(26) Gauss, J.; Stanton, J. F. *J. Phys. Chem. A* **2000**, *104*, 2865.
(27) Quack, M.; Suhm, M. A. *J. Chem. Phys.* **1991**, *95*, 28. Hollenstein, H.; Marquardt, R. R.; Quack, M.; Suhm, M. A. *J. Chem. Phys.* **1994**, *101*, 3588.
(28) Pulay, P.; Fogarasi, G.; Boggs, J. E. *J. Chem. Phys.* **1981**, *74*, 3999.
(29) Maslen, P. E.; Handy, N. C.; Amos, R. D.; Jayatilaka, D. *J. Chem. Phys.* **1992**, *97*, 4233. Miani, A.; Cané, E.; Palmieri, P.; Trombetti, A.; Handy, N. C. *J. Chem. Phys.* **2000**, *112*, 248.
(30) Quack, M. *Faraday Discuss. Chem. Soc.* **1981**, *71*, 359−364 and unpublished results.
(31) Quack, M. *IL Nuovo Cimento B* **1981**, *63B*, 358.
(32) Quack, M. *Annu. Rev. Phys. Chem.* **1990**, *41*, 839.
(33) Quack, M. **1993**, *J. Mol. Struct. 292*, 171. Quack, M.; Kutzelnigg, W. *Ber. Bunsen-Ges. Phys. Chem.* **1995**, *99*, 231.
(34) Lehmann, K. K.; Scoles, G.; Pate, B. H. *Annu. Rev. Phys. Chem.* **1994**, *45*, 241.
(35) Gruebele, M.; Bigwood, R. *Int. Rev. Phys. Chem.* **1998**, *17*, 91.
(36) Scotoni, M.; Boschetti, A.; Oberhofer, N.; Bassi, D. *J. Chem. Phys.* **1991**, *94*, 971. Scotoni, M.; Leonardi, C.; Bassi, D. *J. Chem. Phys.* **1991**, *95*, 8655. Bassi, D.; Menezotti, L.; Oss, S.; Scotoni, M.; Iachello, F. *Chem. Phys. Lett.* **1993**, *207*, 167.
(37) Page, R. H.; Shen, Y. R.; Lee, Y. T. *J. Chem. Phys.* **1988**, *88*, 5362−5376, 4621.
(38) Callegari, A.; Srivastava, H. K.; Merker, U.; Lehmann, K. K.; Scoles, G.; Davis, M. *J. Chem. Phys.* **1997**, *106*, 432.
(39) Callegari, A.; Merker, U.; Engels, P.; Srivastava, H. K.; Lehmann, K. K.; Scoles, G. *J. Chem. Phys.* **2000**, *113*, 10583. Erratum. *J. Chem. Phys.* **2001**, *114*, 3344.

(40) Bray, R. G.; Berry, M. J. *J. Chem. Phys.* **1979**, *71*, 4909.
(41) Reddy, K. V.; Heller, D. F.; Berry, M. J. *J. Chem. Phys.* **1982**, *76*, 2814.
(42) Sibert, E. L., III.; Reinhardt, W. P.; Hynes, J. T. *J. Chem. Phys.* **1984**, *81*, 1115.
(43) Shi, S.; Miller, W. H. *Theor. Chim. Acta* **1985**, *68*, 1.
(44) Lu, D.-H.; Hase, W. L. *J. Phys. Chem.* **1988**, *92*, 3217.
(45) Zhang, Y.; Marcus, R. A. *J. Chem. Phys.* **1992**, *97*, 5283.
(46) Zhang, Y. F.; Klippenstein, S. J.; Marcus, R. A. *J. Chem. Phys.* **1991**, *94*, 7319.
(47) Zhang, Y. F.; Marcus, R. A. *J. Chem. Phys.* **1992**, *96*, 6065.
(48) Iung, C.; Wyatt, R. E. *J. Chem. Phys.* **1993**, *99*, 2261.
(49) Rashev, S.; Stamova, M.; Djambova, S. *J. Chem. Phys.* **1998**, *108*, 4797.
(50) Minehardt, T. J.; Adcock, J. D.; Wyatt, R. E. *Chem. Phys. Lett.* **1999**, *303*, 537.
(51) Rumpf, K.; Mecke, R. *Z. Phys. Chem. B* **1939**, *44*, 299.
(52) Henry, B. R.; Siebrand, W. *J. Chem. Phys.* **1968**, *49*, 5369.
(53) Hayward, R. J.; Henry, B. R.; Siebrand, W. *J. Mol. Spectrosc.* **1973**, *46*, 207.
(54) Halonen, L. *Chem. Phys. Lett.* **1982**, *87*, 221; see also ref 51.
(55) Brodersen, S.; Langseth, A. *Mater. Fys. Skrifter Danske Vid. Selskab* **1956**, *1*, 1.
(56) Brodersen, S.; Christoffersen, J.; Bak, B.; Nielsen, J. T. *Spectrochim. Acta* **1965**, *21*, 2077.
(57) Snavely, D. L.; Walters, V. A.; Colson, S. D.; Wiberg, K. B. *Chem. Phys. Lett.* **1984**, *103*, 423.
(58) Esherick, P.; Owyoung, A.; Plíva, J. *J. Chem. Phys.* **1985**, *83*, 3311.
(59) Plíva, J.; Pine, A. S. *J. Mol. Spectrosc.* **1987**, *126*, 82.
(60) Plíva, J.; Johns, J. W. C.; Goodman, L. *J. Mol. Spectrosc.* **1990**, *140*, 214.
(61) Plíva, J.; Johns, J. W. C.; Lu, Z. *Mol. Phys.* **1996**, *87*, 859.
(62) Cané, E.; Miani, A.; Trombetti, A. *Chem. Phys. Lett.* **1997**, *272*, 83.
(63) Painter, P. C.; Koenig, J. L. *Spectrochim. Acta* **1977**, *33A*, 1003−1018.
(64) Thakur, S. N.; Goodman, L.; Ozkabak, A. G. *J. Chem. Phys.* **1986**, *84*, 6642−6656.
(65) Dübal, H. R.; Quack, M. *Chem. Phys. Lett.* **1981**, *80*, 439; *J. Chem. Phys.* **1984**, *81*, 3779.
(66) Peyerimhoff, S.; Lewerenz, M.; Quack, M. *Chem. Phys. Lett.* **1984**, *109*, 563.
(67) Quack, M. *Chimia* **2001**, *55*, 753.
(68) Fehrensen, B.; Hippler, M.; Quack, M. *Chem. Phys. Lett.* **1998**, *298*, 320.
(69) Hippler, M.; Quack, M. *Chem. Phys. Lett.* **1994**, *231*, 75.
(70) Hippler, M.; Quack, M. *J. Chem. Phys.* **1996**, *104*, 7426.
(71) Hippler, M.; Quack, M. *Ber. Bunsen-Ges. Phys. Chem.* **1997**, *101*, 356.
(72) Ishiuchi, S.; Shitomi, H.; Takazawa, K.; Fujii, M. *Chem. Phys. Lett.* **1998**, *283*, 243.
(73) Riedle, E.; Beil, A.; Luckhaus, D.; Quack, M. *Mol. Phys.* **1994**, *81*, 1.
(74) Snels, M.; Hollenstein, H.; Quack, M. *Chem. Phys. Lett.* **2001**, *350*, 57.
(75) Snels, M.; Hollenstein, H.; Quack, M. *Mol. Phys.* **2002**, *100*, 981.
(76) Rothman, L. S.; Gamache, R. R.; Tipping, R. H.; Rinsland, C. P.; Smith, M.; Benner, D. C.; Devi, V. M.; Flaud, J. M.; Camy-Peyret, C.; Perrin, A.; Goldman, A.; Massie, S. T.; Brown, L. R.; Toth, R. A. *J. Quant. Spectrosc. Radiat. Trans.* **1992**, *48*, 469.
(77) Boublik, T.; Fried, V; Hala, E. *The Vapour Pressures of Pure Substances*; Elsevier: Amsterdam, 1984.
(78) Lias, S. G.; Bartmess, J. E.; Liebman, J. F.; Holmes, J. L.; Levin, R. D.; Mallard, W. G. Ion Energetics Data. In *NIST Chemistry WebBook*; Mallard, W. G., Linstrom, P. J., Eds.; NIST Standard Reference Database 69; National Institute of Standards and Technology: Gaithersburg, MD, March 1998 (http://webbook.nist.gov).
(79) Beyer, T.; Swinehart, D. F. *Commun. ACM* **1973**, *16*, 379.
(80) Boesl, U.; Neusser, H. J.; Schlag, E. W. *Chem. Phys.* **1981**, *55*, 193. Riedle, E.; Knittel, Th.; Weber, Th.; Neusser, H. J. *J. Chem. Phys.* **1989**, *91*, 4555.
(81) Hippler, M.; Pfab, J. *Chem. Phys. Lett.* **1995**, *243*, 500.
(82) Helman, A.; Marcus, R. A. *J. Chem. Phys.* **1993**, *99*, 5002 and 5011.
(83) Bryce-Smith, D.; Longuet-Higgins, H. C. *Chem. Commun.* **1966**, *17*, 593.
(84) Sobolewski, A. L.; Woywod, C.; Domcke, W. *J. Chem. Phys.* **1993**, *98*, 5627.
(85) Iachello, F.; Oss, S. *J. Mol. Spectrosc.* **1992**, *153*, 225.
(86) Mecke, R. *Z. Elektrochem.* **1950**, *54*, 38 and references therein.
(87) Schek, I.; Jortner, J.; Sage M. L. *Chem. Phys. Lett.* **1979**, *64*, 209.
(88) Amrein, A.; Dübal, H. R.; Lewerenz, M.; Quack, M. *Chem. Phys. Lett.* **1984**, *112*, 387.
(89) Lewerenz, M.; Quack, M. *Chem. Phys. Lett.* **1986**, *123*, 197.
(90) Lippert, E. Ph.D. Thesis 1951, Universität Freiburg. Lippert, E.; Mecke, R. *Z. Elektrochem.* **1951**, *55*, 366.
(91) Gross, H.; He, Y. B.; Quack, M.; Schmid, A.; Seyfang, G. *Chem. Phys. Lett.* **1993**, *213*, 122.
(92) Quack, M. *J. Chem. Phys.* **1985**, *82*, 3277.
(93) Bixon, M.; Jortner, J. *J. Chem. Phys.* **1968**, *48*, 715.
(94) Segall, J.; Zare, R. N.; Dübal, H. R.; Lewerenz, M.; Quack, M. *J. Chem. Phys.* **1987**, *86*, 634.
(95) Boyarkin, O. V.; Settle, R. D. F.; Rizzo, T. R. *Ber. Bunsen-Ges. Phys. Chem.* **1995**, *99*, 504.
(96) Snels, M.; Hollenstein, H.; Quack, M.; Cané, E.; Miani, A.; Trombetti, A. *Mol. Phys.* **2002**, *100*, 981.